ON THE CHOICE OF A WINDBREAK POROSITY PROFILE

J. D. WILSON

Meteorology Division, Geography Department, University of Alberta, Edmonton, Alberta, Canada T6G 2H4

(Received in final form 13 August, 1986)

Abstract. Measurements of mean windspeed and turbulence were carried out behind two sections of 50% porous fence differing only in the vertical distribution of their porosity. One section of the fence was uniformly porous, the other relatively dense near the ground and open aloft. Slightly greater mean speed reduction was observed near the ground in the near lee of the section which was dense at ground-level without any detrimental increase in turbulence. However, this advantage was offset by less effective protection in the far lee. These findings are consistent with earlier work by Gandemer (1979) and with the predictions of a numerical model of windbreak flow.

1. Introduction

Artificial porous windbreaks are now in widespread use for many purposes. Several types of porous windbreak are commercially available (e.g., wooden-slotted snow-fence, plastic mesh), and without exception, these are manufactured so as to give a uniform distribution of porosity with height. The intention of this paper is to examine whether or not a vertically-uniform porosity distribution is optimal from the point of view of windspeed reduction.

That a windbreak should be porous in order to prevent the creation of an intensely turbulent wake is beyond dispute. However, even a very porous windbreak, while not causing a lee-side recirculation zone, does cause increased levels of turbulence in a region of the leeward flow as a result of advection and diffusion of kinetic energy away from a region of strong shear-production just above the fence (see Raine and Stevenson, 1977).

It is also widely believed that the flow behind a porous fence is relatively insensitive to the fence construction for a given value of the porosity (but it is more reasonable to expect constancy of the flow for a given value of the fence resistance coefficient (defined later)). Several authors have recommended optimal values of porosity (e.g., Jensen, 1954, porosity $\phi = 35$–40%; Baltaxe, 1967, $\phi = 50\%$). There remain important questions. For example, it is widely believed (van Eimern *et al.*, 1964) that a dense windbreak, while causing greater wind reduction than its more open counterpart, leads to a more rapid rate of recovery towards the unsheltered condition. Defining a 'wind reduction curve' as $\bar{u}(x, z)/\bar{u}_o(z)$ versus x (where $\bar{u}(x, z)$ is the time-average horizontal windspeed, x and z are, respectively, the streamwise and vertical coordinates, and the subscript 'o' denotes a far upstream value), the accepted belief is that the wind reduction curves for the 'more dense' and 'more open' windbreaks cross each other. The 'more dense' windbreak is thought to be less effective overall than the 'more open'.

Recent support for this traditional view has been given by Gandemer (1979), who studied a variety of artificial barriers in a wind-tunnel boundary-layer flow. The

Boundary-Layer Meteorology **38** (1987) 37–49.

artificially-stimulated flow was not described in detail, nor was the ratio H/z_o of fence height to surface roughness length given; the ratio of fence length/height was 24, which is insufficient to yield two-dimensional mean flow. Though Gandemer does not show actual wind reduction curves (i.e., horizontal profiles of $U_+ = \bar{u}(x, z)/\bar{u}_o(z)$), his Figure 3 compares the areas protected to at least a given degree (highly protected, $U_+ \leqq 0.3$; somewhat protected, $U_+ \leqq 0.8$) behind 54% and 20% porous fences of the same height (the fence resistance coefficients were not given but presumably that for the 20% porous fence exceeded that of the 54% fence). The area highly protected ($U_+ \leqq 0.3$) increased as porosity decreased from 54% to 20%. However, the (larger) area within which $U_+ \leqq 0.8$ decreased with decreasing porosity (by a small amount in percentage terms, which raises the question of experimental uncertainty; estimation of the area covered by at least a small wind reduction is strongly affected by small errors in windspeed measurement). This finding implies that the wind reduction curves for 54% and 20% porous fences crossed.

On the other hand, Wilson (1985) examined the results of several relatively modern windbreak fence experiments and found that in these cases a more dense windbreak yielded not only a greater speed reduction, but also a greater range of shelter. This concurred with the prediction of the numerical model of windbreak flow which was the main subject of Wilson (1985).

In view of the conflicting data on the issue of the relationship of wind protection to windbreak porosity, it is important that the instrumental limitations of the early work on shelter be borne in mind, and that the design criteria be reviewed. Furthermore, it is clear that no single type of windbreak gives 'best' protection in all circumstances and by all criteria of performance.

As stated above, the present norm in artificial windbreaks is a uniform porosity profile. However, it has been speculated (e.g., Rosenburg, 1975) that it may be preferable to employ a fence which is relatively open near ground. While this may be desirable in some cases (e.g., to allow cold air drainage), it runs counter to intuition if the purpose is to reduce the near-ground windspeed.

The source of this concept may have been Baltaxe (1967), who reasoned that since one may prevent flow separation on an aerofoil by injecting high speed flow into the boundary layer, one might in a parallel way prevent separation behind a fence by encouraging a near-ground bleed flow. However Baltaxe's inferences regarding the turbulence pattern were based on visual observations of wind vanes, and he apparently did not conclude, as is now generally believed, that a sufficiently porous fence ($\phi > 30\%$ according to Perera, 1981) does not cause separation, and that in the 'quiet zone' in the near lee of both porous and solid fences, the turbulent kinetic energy is reduced below upstream levels (Raine and Stevenson, 1977).

In order to consider the impact of the porosity profile on shelter effectiveness, it is useful to fix the overall porosity and to vary the distribution of porosity with height. Gandemer (1979) presented measurements of protected area behind two variable-porosity fences sharing the same average porosity of 40% (unfortunately there is no direct comparison with a uniformly porous 40% fence). In one case, porosity varied

from 60% at ground-level to 20% at top (open at the ground, 0); in the other case, the porosity varied in the reverse manner (dense at the ground, D). It was found that the highly protected area ($U_+ \leqq 0.3$) behind the D fence exceeded that behind the O fence, and behind the uniformly 54% and 20% porous fences. However considering the larger, but less protected area ($U_+ \leqq 0.8$), the D fence provided a smaller protected area than the O fence or either of the uniformly-porous fences. This means that the wind reduction curve for the D fence crossed the wind reduction curves for the O fence and the uniform 54 and 20% porous fences (and, therefore, presumably would have crossed the curve for a uniform 40% fence).

The next sections will describe the prediction of a numerical model of windbreak flow for the dependence of wind reduction upon the fence porosity profile. Subsequent sections will describe a field experiment which confirms the general pattern suggested by Gandemer and by the flow model.

2. Numerical Prediction of the Effect of Variable Porosity Profile

A full description of the windbreak-flow model is given by Wilson (1985). The model is applicable to a two-dimensional neutrally-stratified mean flow perpendicular to an infinitely-long porous fence. The equations of motion are solved using a second-order closure scheme which has proven useful in many engineering flows and which was adopted without modification. To obtain a prediction of a windbreak flow, it is necessary only to specify the ratio H/z_o and the dimensionless pressure loss coefficient or resistance coefficient k_r* of the fence. Momentum is absorbed at the fence at a rate $k_r \bar{u} |\bar{u}|$, directly simulating the natural process. It was shown that the flow simulation gives a very good prediction of the degree of wind reduction in the near lee, but that the rate of recovery of the wind profile to upstream equilibrium conditions was underestimated.

An overall (bulk) porosity of 50% was adopted for this work. Because the numerical model had been directly verified at this porosity (more correctly, at the value of resistance coefficient $k_r = 2$), it was decided to allow the porosity to vary only modestly from 50%, in the range 30 to 70%. In order to relate porosity to k_r, the empirical relationship given by Hoerner (1965) for a square bar lattice was adopted,

$$k_r = \tfrac{1}{2}\left[\frac{3}{2\phi} - 1\right]^2 .$$

Table I shows the profile of k_r adopted for each of the fences and the corresponding (or intended) porosity.

Results of Simulation:

The total drag on the fence (per unit length) corresponds to the total rate of removal of momentum from the flow (per unit crosswind length). For the case examined

* $k_r \rho u^2$ gives the pressure drop across a sample of given material mounted so as to block a wind tunnel flow of density ρ and velocity u.

TABLE I

Profile of resistance coefficient k_r used in simulation of uniform (U), dense-at-ground (D), and open-at-ground (O) porous fences. The corresponding values of porosity were obtained from Hoerner's formula for a square bar lattice

Height z/H	Fence					
	U		D		O	
	k_r	Local porosity	k_r	Local porosity	k_r	Local porosity
0.05	2.0	0.5	8.0	0.3	0.65	0.7
0.15		0.5	8.0	0.3	0.65	0.7
0.25			3.8	0.4	1.12	0.6
0.35			3.8	0.4	1.12	0.6
0.45			2.00	0.5	2.00	0.5
0.55			2.00	0.5	2.00	0.5
0.65			1.12	0.6	3.8	0.4
0.75			1.12	0.6	3.8	0.4
0.85			0.65	0.7	8.0	0.3
0.95			0.65	0.7	8.0	0.3

($H/z_o = 600$), the dense-at-ground fence (D) extracted only 89% of the momentum extracted by the uniform fence, while its inverted image (O) extracted 105% of the momentum extracted by the uniform fence. However, Figure 1, a vertical profile of the fractional velocity reduction

$$S(x, z) = \frac{\Delta \bar{u}}{\bar{u}_o} = \frac{\bar{u}_o(z) - \bar{u}(x, z)}{\bar{u}_o(z)}$$

at $x/H = 4$ (in the region of minimum speeds), shows that the D and O fences cause, respectively, greater and less speed reduction in the near lee than does the uniform fence. The solid line in Figure 1 gives the observations of Bradley and Mulhearn (1983) for a uniformly porous fence with $\phi = 50\%$, $H/z_o = 600$, and shows that the numerical simulation gives an excellent prediction of the velocity reduction in the near lee.

Figure 2 gives horizontal profiles of fractional speed reduction $S(x, z)$ for $z/H = 0.25$. According to the model, the region of improved velocity reduction behind the D fence extends only as far downstream as $x/H \cong 7$, beyond which the D fence is slightly less effective than the uniform one. These predictions are in qualitative agreement with the observations reported by Gandemer, and there is a strong silimarity between the model prediction and the observations of Figure 4(c).

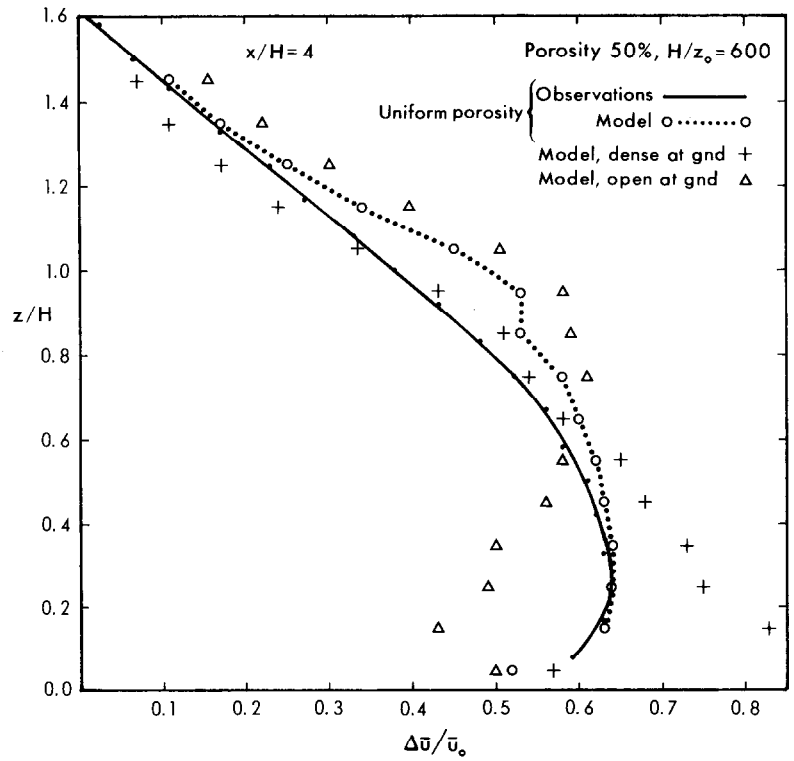

Fig. 1. Vertical profiles of fractional wind reduction in the near lee ($x/H = 4$) of 50% porous shelter fences having $H/z_o = 600$. The solid curve gives the field observations of Bradley and Mulhearn (1983) and the dotted curve gives the model prediction for that experiment. Also shown are predictions for the fences described in Table I having height-dependent porosity.

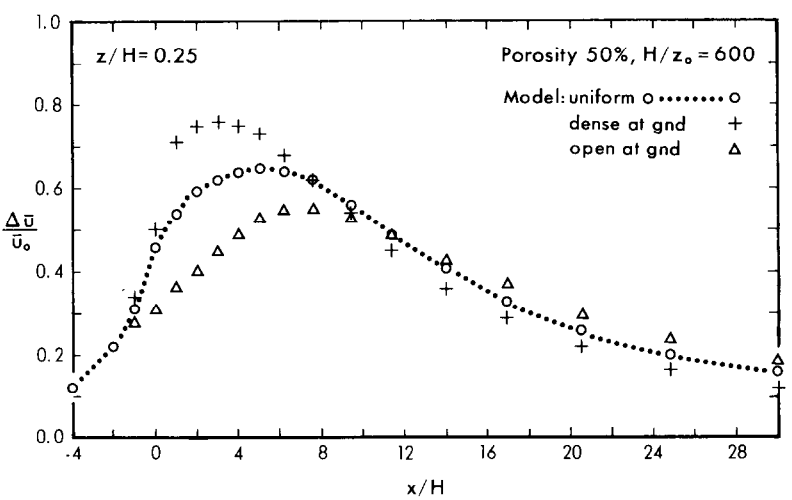

Fig. 2. Horizontal profiles of fractional velocity reduction at $z/H = \frac{1}{4}$ according to the numerical model.

3. Experiment on the Effect of Variable Porosity Profile

3.1. Site and Experimental Procedure

The experiment was carried out in a large field of stubble having a surface roughness length of about $z_o = 0.015$ m at Ellerslie, Alberta, Canada, during the autumn of 1985 and spring of 1986. The field slope was estimated to be $< 1\%$ (perpendicular to the fence) and the uniformity of the upstream fetch was broken only by a side road at 300 m.

The fence was 100 m long, 1.12 m high (so that the ratio of height to surface roughness

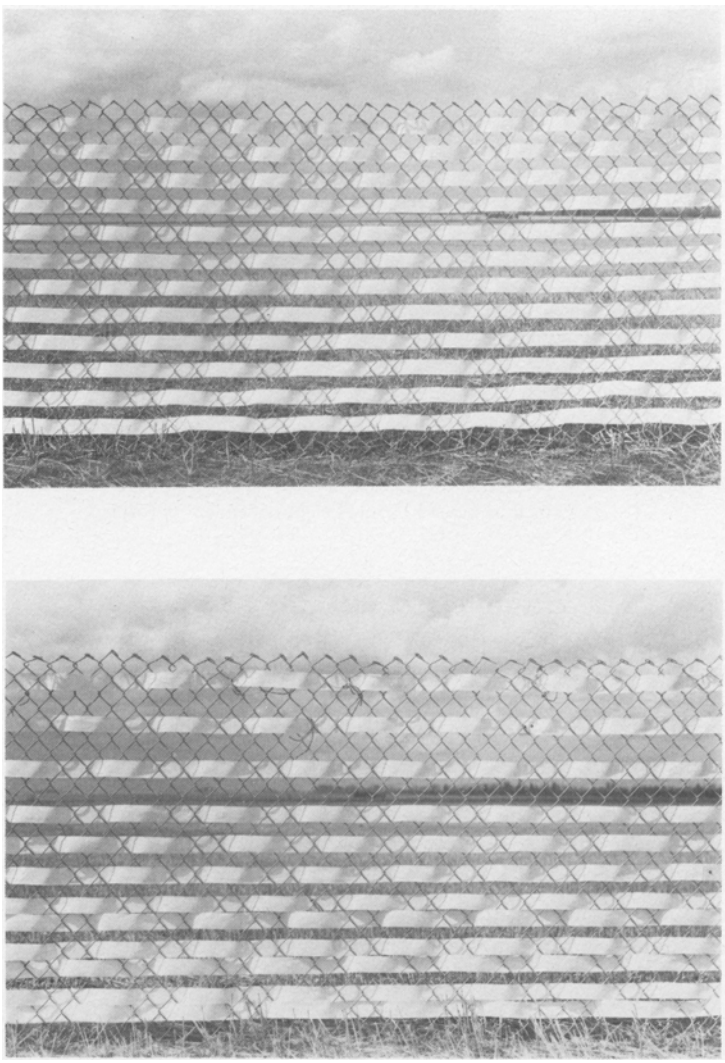

Fig. 3. Photograph of the two sections of 50% porous fence. The '*D*-side' is more dense at ground-level and more open aloft than the uniformly porous '*U*-side'.

was $H/z_o = 75$), and was constructed by weaving plastic tape into diamond mesh wire netting. The overall porosity was 50%. Half of the fence (hereafter the '*U*-side') was woven so as to be uniformly porous, while the adjoining half (the '*D*-side') was woven (using the same quantity of tape) to give higher and lower densities than the *U*-side at ground and at the fence top, respectively (Figure 3).

Mean windspeeds were measured with Climet 011–4 cup anemometers which had been calibrated against a pitot tube and pressure transducer (the latter being first calibrated against a sensitive manometer) prior to the experiment. A tower 30 m upstream from the fence supported 4 or 5 cup anemometers, a wind vane, and 2 shielded thermocouple pairs. To the lee of the fence, windspeeds were measured near the mid-line through the *U* and *D* sections on adjustable tripods.

Signals from the instruments were sampled continuously by a data-logger; 30-min periods, which were acceptable from the point of view of wind-direction, standard deviation of wind direction, and near-neutrality, were extracted.

Turbulence measurements were made using 2 single-axis sonic anemometers* (path-length 0.1 m). Signals from the sonic anemometers were passed through low pass filters having power gain (1, 1, 0.60, 0.22, 0.082, 0.035, 0.011) at frequencies (0, 10, 20, 30, 40, 50, 70 Hz), respectively, digitized at 20 Hz, and stored on floppy diskettes for subsequent analysis.

3.2. Results: mean flow

The data to be presented were selected using the criteria that:

(i) the average wind direction over the 30-min period should be within $\pm 10°$ of the normal to the fence with a standard deviation not exceeding 15°.

(ii) The approaching windspeed at $z = 5.5$. m should exceed 5 m s^{-1}.

(iii) The magnitude of the temperature difference between $z = 0.3$ m and $z = 5.3$ m on the upstream tower should not exceed 1 °C.

Almost all the runs accepted were in slightly unstable stratification, and the above limitations on the wind and temperature profiles correspond to the restriction that $|L| \gtrsim 60$ m, i.e., $H/|L| \lesssim 0.02$. The experiment was suspended during snowfall and snow cover.

As expected, windspeeds normalized by a reference value such as the top windspeed measurement on the tower were relatively invariant. Use of more stringent selection criteria would have further reduced the variability in the normalized windspeeds, but would have yielded fewer usable periods.

Leeward windspeeds were measured at heights of H, $H/2$, and $H/4$. Figure 4 gives the horizontal profile at each of these heights of the fractional cup windspeed reduction behind the *U* and *D* fences. The maximum fractional reduction at $z/H = \frac{1}{2}$ behind the *U* fence is about 0.6. Wilson (1985) suggested the formula

$$\frac{\Delta \bar{u}}{\bar{u}_o} = 0.19 \ln (k_r) + 0.42,$$

* Campbell Scientific CA27, Campbell Scientific Inc., Logan, Utah.

for the maximum fractional speed reduction at $z/H = 0.6$. The resistance coefficient of the uniform fence was not measured, but would be expected to lie above $k_r = 2.0$ (square bar lattice, $\phi = 50\%$, plus underlying very porous round-bar lattice). The formula gives $\Delta\bar{u}/\bar{u}_o = 0.55$, 0.63 for $k_r = 2, 3$. These values bracket the observed reduction.

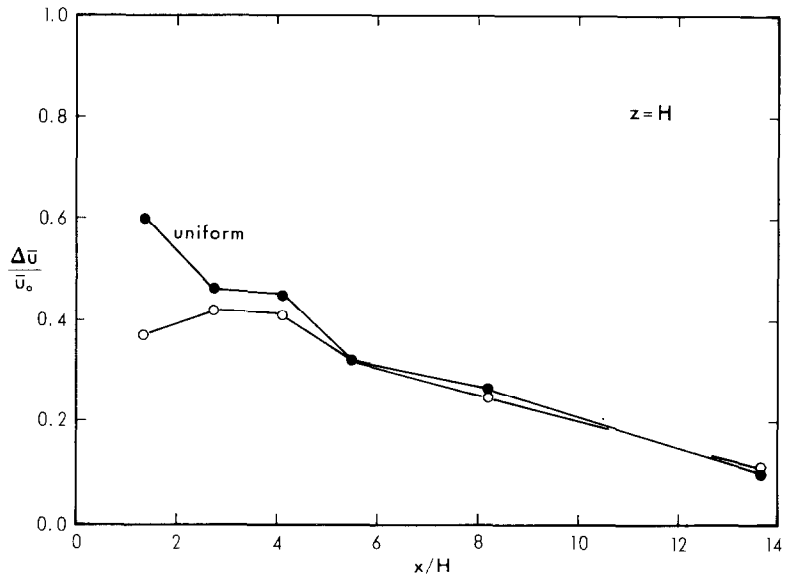

Fig. 4a.

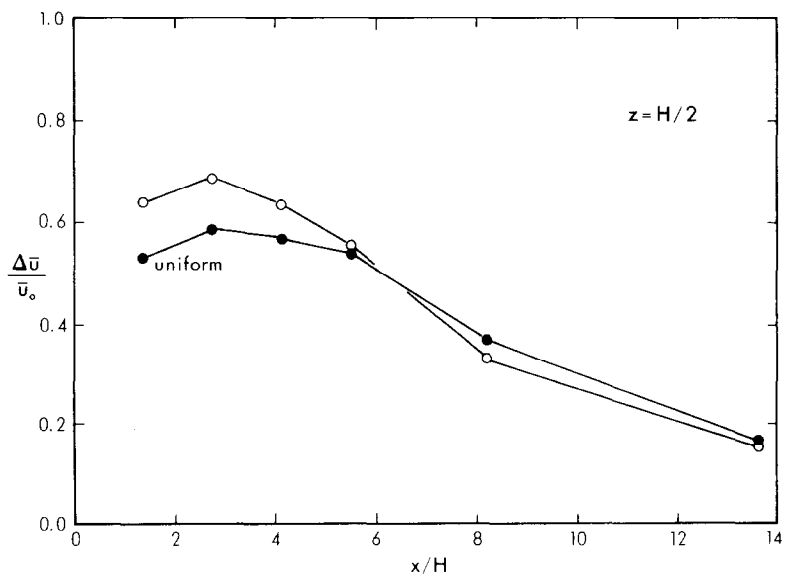

Fig. 4b.

Fig. 4. Horizontal profiles of fractional wind reduction $\Delta\bar{u}/\bar{u}_o$ at heights (a) $z/H = 1$, (b) $z/H = \frac{1}{2}$, (c) $z/H = \frac{1}{4}$.

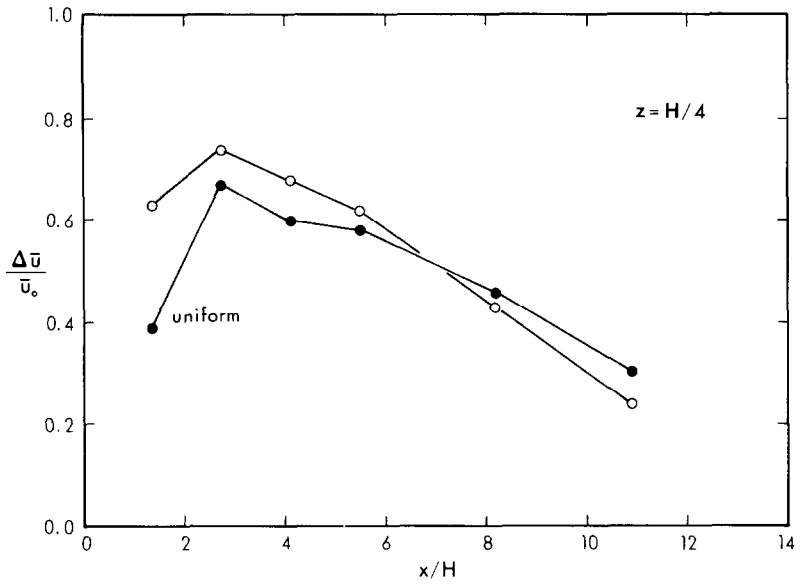

Fig. 4c.

As might be expected, windspeed near $z = H$ is higher behind the D-side (which is relatively open at $z = H$) than behind the U-side; however, the difference is not very significant beyond about $x/H = 2$. At $z/H = \frac{1}{2}$ and $\frac{1}{4}$, windspeeds behind the D-side are noticeably lower than behind the U-side out to about $x/H = 7$, beyond which the uniform fence is slightly more effective. As noted earlier, there is good qualitative agreement of the experimental fractional reduction curve with the model prediction (Figure 2). The advantage of the D fence relative to the U fence is very modest – about an extra 10 to 15% speed reduction in the near lee of the fence – and is partially offset by less effective shelter in the far lee.

3.3. Results: Turbulence

Turbulence measurements behind solid and uniformly porous windbreaks have been presented by Hagen and Skidmore (1971), Raine and Stevenson (1977), Ogawa and Diosey (1980), and Finnigan and Bradley (1983). The general features recognized are:

(i) A 'quiet zone' of reduced velocity variance in the near lee of the windbreak, bounded approximately by a line from fence-top to the ground at $x/H \sim 8$. The extent of suppression of turbulence depends on porosity; Hagen and Skidmore reported a 50% reduction in $\overline{u'^2}$ behind a solid fence, and a 90% reduction behind porous fences.

(ii) A 'turbulent zone' of increased velocity variance advecting and spreading downwind from a point near the top of the fence (a consequence of the very strong wind shear caused by reduced velocity near the ground and compensating increased velocity above the fence).

Figures 5 and 6 give horizontal profiles of the variance ratios $\overline{w'^2}(z)/\overline{w_o'^2}(z)$, $\overline{v'^2}(z)/\overline{v_o'^2}(z)$ formed from simultaneous upstream and downstream measurements.

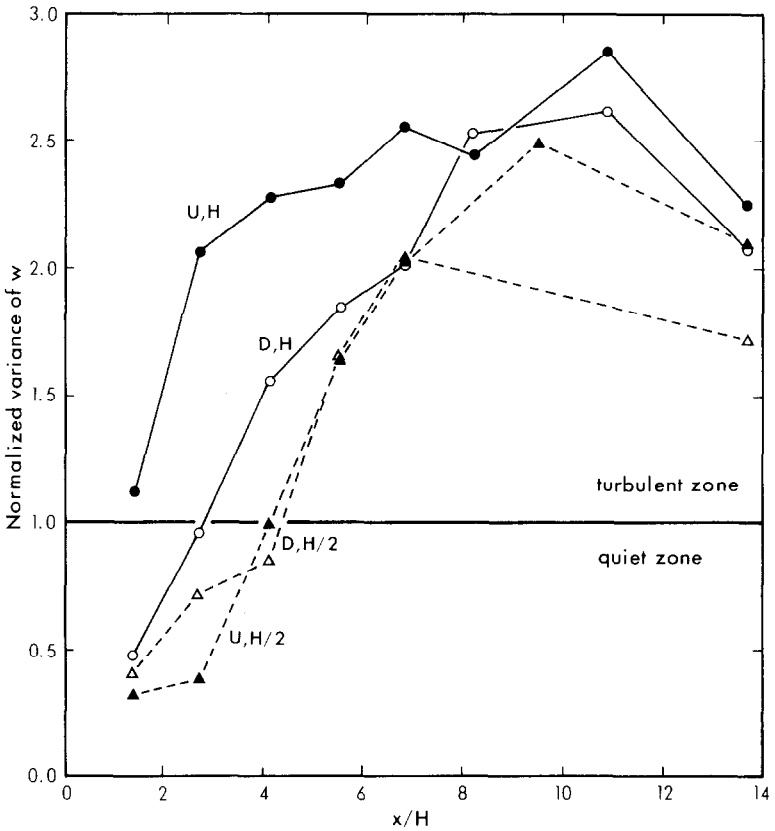

Fig. 5. Horizontal profiles of $\overline{w'^2}/\overline{w_o'^2}$ at $z/H = 1$ (●, ○) and $z/H = \frac{1}{2}$ (▲, △) behind the U and D fences.

These velocity variances are for 4.17 min periods, which are shorter than is usual, but adequate for seeing important differences from place to place about the fences.

The quiet zone is discernible in both the v and w components. The U and D fences cannot be distinguished in the case of the v component. However, the quiet zone in $\overline{w'^2}$ is deeper behind the D fence, shows a marginally less degree of reduction in $\overline{w'^2}$ at $z/H = \frac{1}{2}$, and extends downstream about the same distance as behind the U fence. The most striking difference between the two fences is the steeper increase in $\overline{w'^2}$ at $z = H$ behind the U fence (presumably because the U-side is more dense at $z = H$ than the D-side. These figures show the general pattern expected from earlier measurements (except that Hagen and Skidmore found increased vertical velocity variance at $z/H = \frac{1}{2}$), and indicate that one could hardly choose one fence from the other on the basis of their effect on the turbulent velocity variances.

Velocity power spectra have been calculated from the recorded velocity series, using the Fast Fourier Transform method applied to 4096 data points (204.8 s). These spectra have certainly been degraded by aliasing, but faster sampling or sharper filters were not

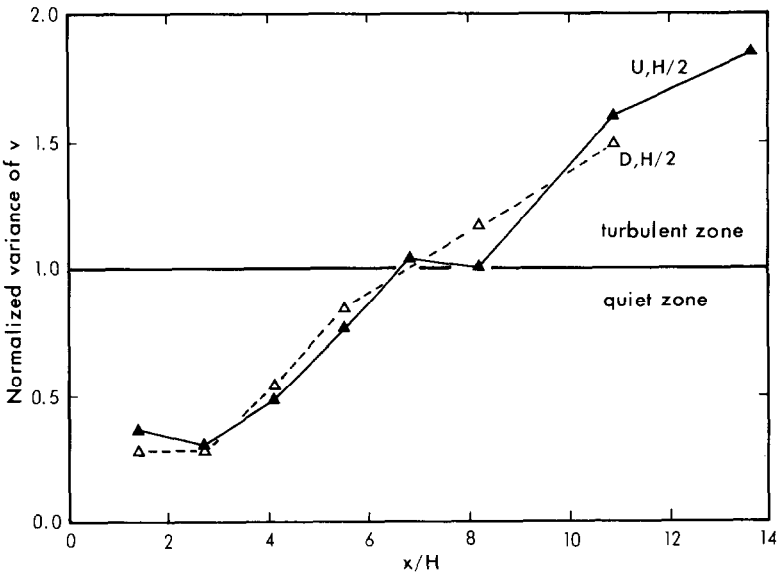

Fig. 6. Horizontal profiles of $\overline{v'^2}/\overline{v_o'^2}$ at $z/H = \frac{1}{2}$ behind the U and D fences.

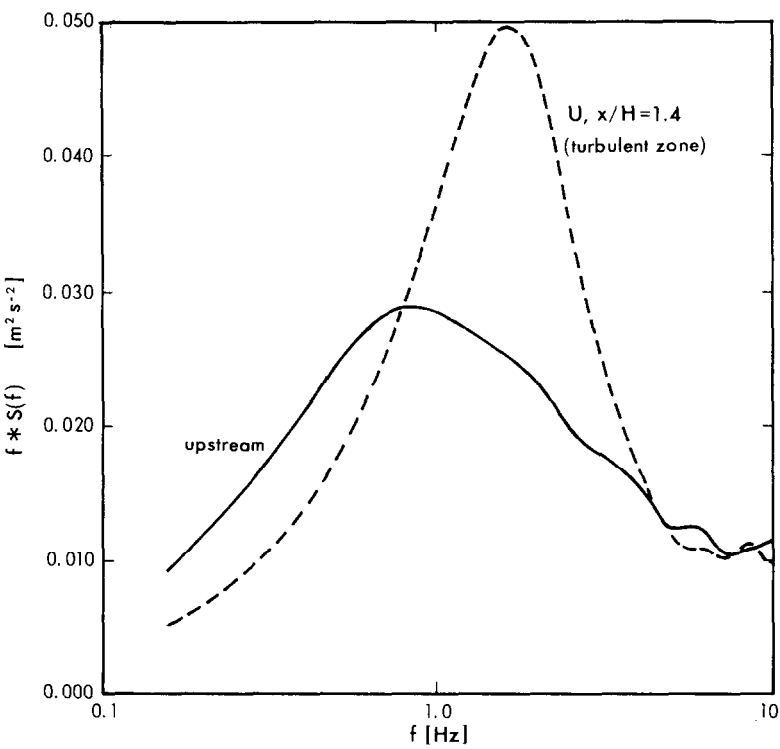

Fig. 7. Vertical velocity spectra at $z/H = 1$. (a) Upstream (———) and at $x/H = 1.4$ behind U-side (– – – – –). (b) At $x/H = 1.4$ behind U-side (– – – – –) and D-side (. . . . .).

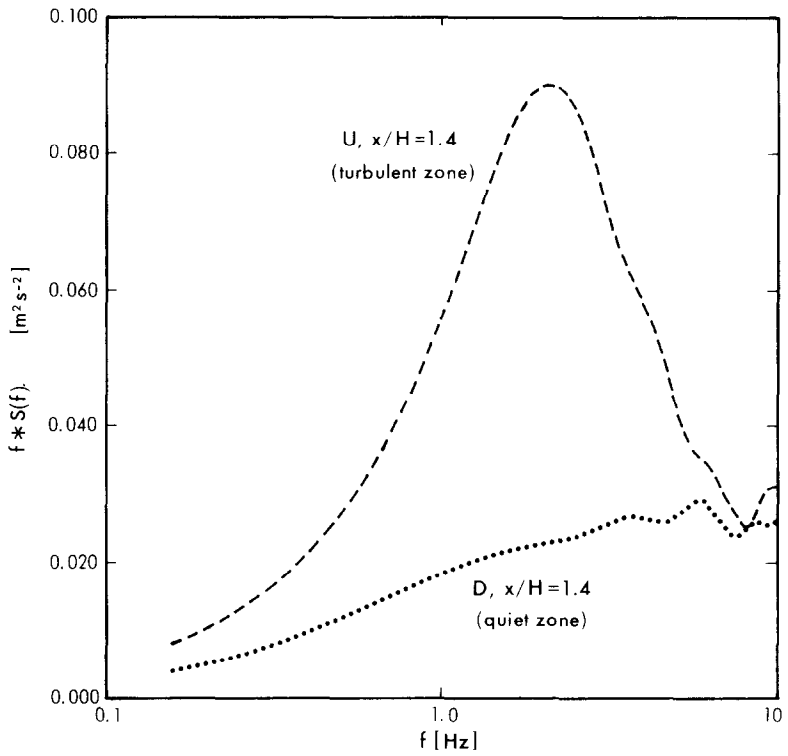

Fig. 7b.

available options. In spite of the aliasing, major changes in the spectra can be distinguished. No attempt has been made to scale the spectra to compare results at different heights or to normalize for the effect of mean velocity $\bar{u}$, and the analysis has simply been used to discriminate the shape of simultaneous raw spectra ($fS(f)$ versus $\ln f$, where $S(f)$ is the spectral power density [$m^2\ s^{-2}/Hz$]) measured at pairs of points in the flow.

Figures 7(a) and 7(b) allow comparison of $\overline{w'^2}$ spectra at $z = H$ upstream, and at $x/H = 1.4$ behind the U and D sides. Note that at this location behind the U fence, one is in the zone of increased variance, but behind the D fence, one is in the quiet zone (Figure 5). The spectral peak behind the fences is shifted to a higher frequency relative to the approach spectrum (whereas Ogawa and Diosey found that the peak frequency of the $\overline{w'^2}$ spectrum was displaced downward in the turbulent zone at $z = H$ behind a solid fence with $H/z_o \sim 63$), and the shift is perhaps greater behind the D fence. By $x/H = 14$, the $\overline{w'^2}$ spectral shapes were the same at all three positions (approach, lee of U, lee of D).

Spectra of $\overline{w'^2}$ at $z/H = \frac{1}{2}$ were grossly distorted by aliasing, but the problem was less severe for the v-component at $z/H = \frac{1}{2}$. It was found that at all downstream distances, the $\overline{v'^2}$ spectra at $z/H = \frac{1}{2}$ behind the U and D sides were indistinguishable and had the same shape as the approach spectrum (with altered variance).

4. Conclusion

Differences in wind reduction and turbulence behind the two fences are fairly slight. Mean windspeed is reduced somewhat more effectively (an additional 10 to 15%) near ground in the near lee ($x/H \lesssim 7$) of the fence which is dense at the ground, with no apparent penalty in the turbulent field but with reduced effectiveness at larger distances relative to the uniform fence. These findings are in qualitative agreement with the wind-tunnel data of Gandemer (1979) and with simulations using the numerical model of Wilson (1985) with $H/z_o = 600$. To date, the author has been unable to simulate this experiment with $H/z_o = 75$. The qualitative similarity between the experimental results with $H/z_o = 75$ and the model results with $H/z_o = 600$ provides some justification for the assumption that the patterns observed may be expected to hold for fences having much larger H/z_o.

For some purposes (e.g., sheltering stock) the small improvement in wind reduction in the near lee of the variable-porosity fence may be worthwhile (since it requires no extra material). However, in general it seems hardly worthwhile to depart from a uniform porosity profile.

Acknowledgements

This work was supported in part by the Natural Sciences and Engineering Research Council of Canada.

References

Baltaxe, R.: 1967, 'Air Flow Patterns in the Lee of Model Windbreaks', *Arch. Meteorol. Geophys. Bioklimatol.*, Ser. B, Band 15, Heft 3.

Bradley, E. F. and Mulhearn, P. J.: 1983, 'Development of Velocity and Shear Stress Distributions in the Wake of a Porous Shelter Fence', *J. Wind Eng. Ind. Aerodyn.* **15**, 145–156.

Finnigan, J. J. and Bradley, E. F.: 1983, 'The Turbulent Kinetic Energy Budget Behind a Porous Barrier: an Analysis in Streamline Coordinates', *J. Wind Eng. Ind. Aerodyn.* **15**, 147–168.

Gandemer, J.: 1979, 'Wind Shelters', *J. Ind. Aerodyn.* **4**, 371–389.

Hagen, L. J. and Skidmore, E. L.: 1971, 'Turbulent Velocity Fluctuations and Vertical Flow as Affected by Windbreak Porosity', *Trans. ASAE* **14**, 634–637.

Hoerner, S. F.: 1965, 'Fluid Dynamic Drag', in S. F. Hoerner (ed.), Library of Congress Catalog Card Number 64–19666.

Jensen, M.: 1954, *Shelter Effect*, The Danish Technical Press, Copenhagen, 1954.

Ogawa, Y. and Diosey, P. G.: 1980, 'Surface Roughness and Thermal Stratification Effects on the Flow Behind a Two-Dimensional Fence. I: Field Study', *Atm. Environ.* **14**, 1301–1308.

Perera, M. D. A. E. S.: 1981, 'Shelter Behind Two-Dimensional Solid and Porous Fences', *J. Wind Eng. Ind. Aerodyn.* **8**, 93–104.

Raine, J. K. and Stevenson, D. C.: 1977, 'Wind Protection by Model Fences in a Simulated Atmospheric Boundary Layer', *J. Ind. Aerodyn.* **2**, 159–180.

Rosenburg, N. J.: 1975, 'Windbreak and Shelter Effects', in: L. P. Smith, (ed.), *Progress in Biometeorology, Division C, Progress in Plant Biometeorology*, Vol. I, pp. 108–134, Swets and Zeitlinger (pub.) Amsterdam.

van Eimern, J., Karschon, R., Razumova, L. A., and Robertson, G. W.: 1964, *Windbreaks and Shelterbelts*, World Meteorological Organization Tech. Note, No. 59.

Wilson, J. D.: 1985, 'Numerical Studies of Flow Through a Windbreak', *J. Wind Eng. Ind. Aerodyn.* **21**, 119–154.